A STUDY ON THE EFFECT OF GPS ACCURACY ON A GPS/INS KALMAN FILTER

King Tin Leung * **James Whidborne** * **David Purdy** **
Alain Dunoyer *** **Robert Williams** *

* *School of Engineering, Cranfield University, Cranfield, UK*
** *Engineering Systems Department, Cranfield University, Shrivenham, UK*
*** *Jaguar Land Rover, Whitley, Coventry, UK*

Abstract: In this paper, a Kalman Filter (KF) is used to fuse the Inertial Navigation System (INS) and Global Positioning System (GPS) for the problem of estimating ground vehicle dynamics. Perfect unbiased measurements of the two sensors are extracted from a simulation using IPG CarMaker at a rate of 1 ms to represent a pseudo-analogue signal. Noise is added to the INS and GPS measurements, and then sampled at 100 Hz and 1 Hz respectively. The sampled signals are integrated in the KF and estimated states are compared with the perfect measurements. Results have shown that bias prediction in an INS is achievable using a KF, but highly dependent on the accuracy of GPS. This study enables guided chart to be produced to aid designers to choose the types of GPS (i.e. sampling rate and variance) against their error criterion.

Keywords: Kalman Filter, GPS/INS, vehicle dynamics, integration, error criterion

1. INTRODUCTION

Nowadays, modern vehicles are equipped with numerous computer control systems, e.g. Anti-lock Braking Systems (ABS) and Electronic Stabilisation Programs (ESP). Many of these systems have been proved effective and have become a standard feature on production vehicles. It can be foreseen that in the coming future, more variety of control systems will be available. However, for effective control, accurate and reliable measurements are required. Dynamic measurements in Inertial Navigation System (INS) for vehicle motion have bias, which causes numerical drifting when rate and acceleration signals are integrated. A potential solution for this problem is by combining the Global Positioning System (GPS) with the INS. Since GPS provides information related to vehicle motion, the biases of the INS can be estimated. During GPS sampling time and outages, the corrected INS measurements are integrated. Fusing the two sensors in this manner utilises the strength of both while compensating for their weaknesses.

There are numerous ways of integrating GPS and INS for better estimations, however, out of these methods, the Kalman Filter (KF) appears to be the most commonly used. This is because KF estimation is simpler, more computational efficient and easier to implement, when compared with others. Most of these KFs are devoted to navigation estimation problem rather than vehicle dynamic predictions. In either case, GPS is used to correct the INS errors when it is available. Between each sampling time and during outages, INS is integrated. However, these integrated states tend to drift off with time. In terms of navigation, one solution to counter this issue is to model the INS error more precisely (Nassar and El-Sheimy, 2006) or include a multiple switching KF model to accommodate different scenarios (Cho, Kim, Cho and Choi, 2007). Another solution is to involve more sensors in the KF (Gao, Petovello and Cannon, 2007) so states are constrained by other measurements. Alternatively, the gap created by the absence of GPS can be filled by some bridging methods (Nassar, Niu and El-Sheimy, 2007).

In the study of vehicle dynamic control, GPS/INS integration is particular useful for obtaining states through estimations when they are not available from sensor measurements. GPS and INS are integrated in a Kinematic KF (KKF) to predict biases in INS, estimating wheel slips and slip angles (Bevly, Gredes and Wilson, 2002). Using these slippages, the tyre cornering stiffness can be predicted through a linear or non-linear tyre model (Bevly, Ryu and Gredes, 2006). With extra information on the vehicle parameters, the KF can be structured as a Model-based KF (MKF) to improve state estimations (Anderson and Bevly, 2004).

Whether the KF is used in navigation or dynamic estimations, GPS can be used as the important source of reference. The quality of predictions relies solely on the accuracy of the GPS. It is, thus, important to know the level of influence that GPS has on KFpredictions.

This paper looks at the effect of GPS accuracy and sampling rate on the KF performance.

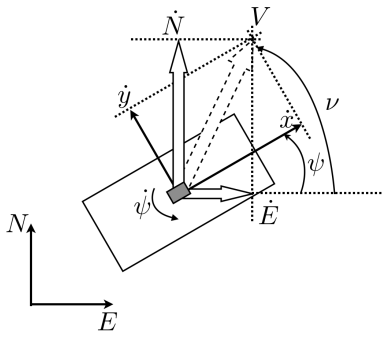

Fig. 1. Plan view showing the velocities vectors in b-frame and e-frame, also the resultant velocity.

2. THEORETICAL BACKGROUND

As described in the introductory section, the INS and GPS can be combined to enhance predictions. To achieve this, the INS measurements must be aligned with the GPS measurements.

The majority of the INS used in ground vehicles nowadays are strapdown sensors, consisting of 3 accelerometers and 3 gyroscopes (or gyros). This type of sensor moves and orientates with the vehicle, so the accelerometers and the gyros measure the accelerations (A_x, A_y) and rotational rate ($\dot{\psi}$, $\dot{\theta}$, $\dot{\varphi}$), respectively, in the vehicle body frame (b-frame). The GPS, however, is referenced to the earth centred axes, measuring the positions (E, N, U) and velocities ($\dot{E}$, $\dot{N}$) in the earth frame (e-frame).

To integrate the two measurements, the INS accelerations are converted to velocities ($\dot{x}$, $\dot{y}$) in the b-frame, which have the following relationships:

$$A_x = \ddot{x} - \dot{y}\dot{\psi} \tag{1}$$

$$A_y = \ddot{y} + \dot{x}\dot{\psi} \tag{2}$$

The velocities in the b-frame and e-frame, therefore, can be related through the resultant velocity vector, V , as shown in equation 3 and Figure 1.

$$V^2 = \dot{x}^2 + \dot{y}^2 = \dot{E}^2 + \dot{N}^2 \tag{3}$$

The vehicle sideslip, β, can be determined by equation 4 and it can be used to map the GPS velocities onto the b-frame.

$$\nu = \tan^{-1}\left(\frac{\dot{N}}{\dot{E}}\right)$$

$$\beta = \nu - \psi \tag{4}$$

$$\begin{cases} \dot{x} = \sqrt{\dot{E}^2 + \dot{N}^2}\cos\beta = \dot{x}_{gps} \\ \dot{y} = \sqrt{\dot{E}^2 + \dot{N}^2}\sin\beta = \dot{y}_{gps} \end{cases} \tag{5}$$

When the vehicle is travelling on a straight road, the heading angle described by the GPS is in the same direction as the vehicle is pointing, i.e V is in-line with $\dot{x}$. Thus, the heading will be the same as the yaw angle.

3. METHODOLOGY

This study looks at the effect of GPS on INS bias prediction using a virtual vehicle under various simulated manoeuvres.

Table 1. Types of errors in sensors

Type of error	Mathematical model
Uncorrelated white noise	$x_w = p$ where p is a normally distributed random variable
Exponential correlated noise	$x_{exp} = x_{exp(0)}\left(1 - e^{-at}\right)$ where $\alpha = \frac{1}{\tau}$, τ is the time constant
Random walk	$x_{rw} = \int p$
Scale factor error	$x_s = s\,(1 + x)$ where s is the scale factor
Quantization error	$x_q = q \cdot round\left(\frac{x}{q}\right) - x$ where q is the quantization level
bias	$x_b = b$ where b is a constant bias

Table 2. INS error in simulation

	Types of error	Value
Accelerometer x	Bias	0.3829 ms^{-1}
	White noise	0.0036
Accelerometer y	Bias	-0.3369 ms^{-1}
	White noise	0.0036
Gyro	none	none

Table 3. GPS receivers accuracy

GPS grade	Price range [1]	Accuracy [2]
Survey	> 12000	0.01 (0.01)
Mapping	500 12000	2 5 (0.10)
Consumer	< 500	15 20 (0.50)

3.1 GPS and INS measurements

GPS and INS measurements are simulated by attaching a sensor at the centre of gravity of the virtual vehicle. The resultant longitudinal and lateral acceleration of the sensor in the body axes form the INS measurements, while the velocities and positions of the sensor in the earth axes correspond to the GPS measurements.

The data for the GPS and INS are captured at 1 kHz to simulate a pseudo-analogue signal before sampling at 1 Hz and 100 Hz respectively. Errors are added into this signal in MatLab and Simulink. These errors are shown in table 1 and can be simulated as described by (Bhatti, Ochieng and Feng, 2007) and by (Grewal, Weill and Andrews, 2007).

In this simulation, the gyro readings are assumed to be error-free. The accelerometers are added with whitenoise, quantization error and biases, see Table 2.

For the GPS in the simulation, its accuracy and sampling rate are varied according to three types of receivers in the market. They are the survey grade, the mapping grade and the consumer grade. Table 3 summaries their precision and price (Wing, Eklund and Kellogg, 2005). GPS sampling rates vary according to the needs of designer, they vary from 0.2 Hz up to 100 Hz. Typical consumer grade GPS has a rate of 1 Hz.

3.2 Kalman Filter Implementation

In general, there are two types of KF, namely the KKF and the MKF. Both KFs share the same formulation, which includes a two-stage process: prediction and correction.

Given a plant with disturbance, w, at the input and noise, v, at the output. It can be approximated with a set of system equations in continuous state space:

$$\dot{x} = Ax + Bu + Gw \tag{6}$$
$$z = Cx + v \tag{7}$$

or discretised state space, which are used in KF:

$$x_{k+1} = \Phi_k x_k + \Delta_k u_k + \Gamma_k w_k \tag{8}$$
$$z_{k+1} = H_k x_k + v \tag{9}$$

In the prediction stage, see equation 10 and 11, states, $\hat{x}_{k+1|k}$, are first predicted with the current estimates, $\hat{x}_{k|k}$, and inputs, u_k. The estimation covariance, $P_{k+1|k}$, is also updated with the current $P_{k|k}$ and process covariance, Q_k.

$$\hat{x}_{k+1|k} = \Phi \hat{x}_{k|k} + \Delta u_k \tag{10}$$
$$P_{k+1|k} = \Phi P_{k|k} \Phi^T + \Gamma Q_k \Gamma^T \tag{11}$$

In the correction stage, the Kalman gain, K, is obtained using $P_{k+1|k}$ and the measurement covariance, R, equation 12. The corrected state, is updated, $\hat{x}_{k+1|k+1}$, using K and the innovation (the difference between the measurement and the predicted states, $z - H_k x_{k+1|k}$), equation 13. Lastly, $P_{k+1|k+1}$ is modified through equation 14.

$$K_k = P_{k+1|k} H (H P_{k+1|k} H^T + R_k)^{-1} \tag{12}$$
$$\hat{x}_{k+1|k+1} = \hat{x}_{k+1|k} + K(z_{k+1} - \hat{z}_{k+1}) \tag{13}$$
$$P_{k+1|k+1} = (I - K_k H) P_{k+1|k} \tag{14}$$

As discussed in the previous section, INS has dynamic equations as equation 1 and 2. Assuming the accelerometer measurements are corrupted by biases, δ_x and δ_y, and white noise only,

$$A_x = \ddot{x} - \dot{y}\dot{\psi} + \delta_x + w_x \tag{15}$$
$$A_y = \ddot{y} + \dot{x}\dot{\psi} + \delta_y + w_y \tag{16}$$

With estimated states being, $[\dot{x}\ \delta_x\ \dot{y}\ \delta_y]^T$, equation 15 and **??** can be rearranged as:

$$\ddot{x} = \dot{y}\dot{\psi} - \delta_x + A_x + w_x \tag{17}$$
$$\ddot{y} = -\dot{x}\dot{\psi} - \delta_y + A_y + w_y \tag{18}$$

The above equation is non-linear, therefore, an Extended KF (EKF) is applied. In an EKF, the system is linearised about a point at a step of 10 ms. The discretised state space model for the INS, Φ_k, G_k, Γ_k and H_k, is therefore:

$$\Phi_k = \begin{bmatrix} 1 & -T_s & \hat{\dot{\psi}}_k T_s & 0 \\ 0 & 1 & 0 & 0 \\ -\hat{\dot{\psi}}_k T_s & 0 & 1 & -T_s \\ 0 & 0 & 0 & 1 \end{bmatrix}, G_k = \begin{bmatrix} T_s & 0 \\ 0 & 0 \\ 0 & T_s \\ 0 & 0 \end{bmatrix}$$

$$\Gamma_k = \begin{bmatrix} T_s & 0 \\ 0 & 0 \\ 0 & T_s \\ 0 & 0 \end{bmatrix}, H_k = \begin{bmatrix} 1 & 0 & 0 & 0 \\ 0 & 0 & 1 & 0 \end{bmatrix} \tag{19}$$

The measurement for this EKF is taken from equations 5, in which the sideslip, β, is determined from the difference between the GPS heading and integrated gyro signal.

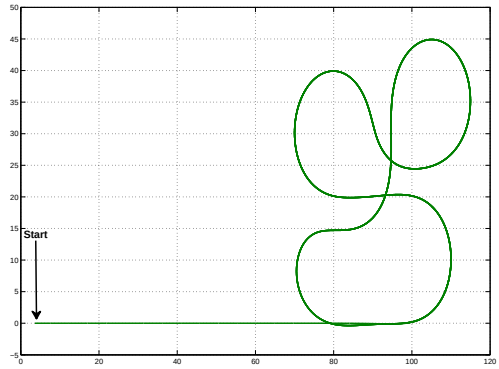

Fig. 2. The plan view for the virtual course.

In order for the EKF to perform effectively, the choice of the covariance matrices, P, Q and R, are important. In this particular EKF, they are definedas:

$$\begin{cases} Q = diag[\sigma^2_{A_x}, \sigma^2_{A_y}] \\ R = diag[\sigma^2_{\dot{x}_{gps}}, \sigma^2_{\dot{y}_{gps}}] \\ P_{0|0} = diag[\sigma^2_{\dot{x}_{gps}}, \delta^2_{x|0}, \sigma^2_{\dot{y}_{gps}}, \delta^2_{y|0}] \end{cases} \tag{20}$$

In reality, all the above parameters will be unknown. Testing and tuning for each sensor is therefore essential before implementation.

3.3 The simulation

Parameters of a Jaguar Sedan are pre-specified as the vehicle model in the simulation, which is then carried out in IPG CarMaker.

Two manoeuvres are simulated while the GPS precision and sampling rate is varied. Each manoeuvre is simulated ten times to obtain an average for the result. Manoeuvre 1 describes a car accelerating from 0 m/s to 5 m/s for the first 100 m before entering the cornering manoeuvre. The entire simulation time is 300 s. The virtual course used for this simulation is as shown in Figure 2. Manoeuvre 2 describes a car travelling on a straight road for 300 s., accelerating from 0 m/s to 5 m/s.

4. RESULTS AND DISCUSSIONS

4.1 Effect without KF prediction

Using the errors specified in Table 2, simulations are performed. Without the EKF, the integrated longitudinal velocity, $\dot{x}$, results in drifting as seen in Figure 3. With a GPS variance of 5.6e-4 at 1 Hz, the EKF is able to correct the velocity, see Figure 4, by estimating the bias in the INS as shown in Figure 5.

4.2 Effect of GPS sampling rate

Preliminary results show that the EKF is predicting and converging onto the bias quickly. To see the effect of different sampling rates, the variance of the GPS signal is fixed at 5.6e-4. The sample rate used for the GPS varies from 0.1 Hz to 100 Hz. For each sampling rate, the error

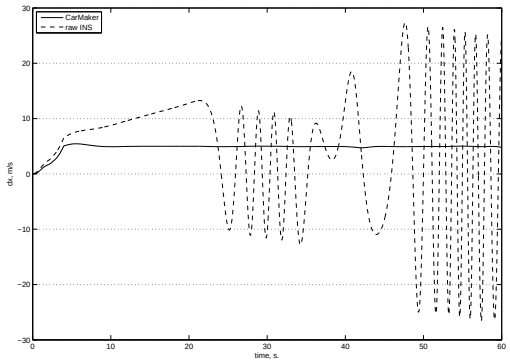

Fig. 3. Longitudinal velocity without EKF

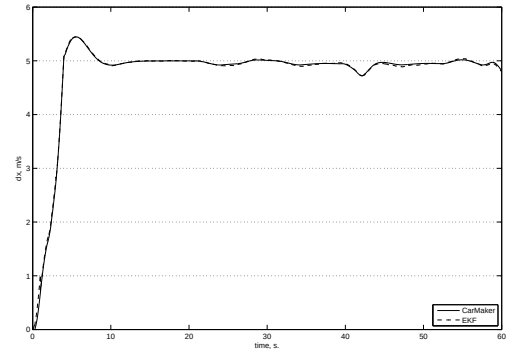

Fig. 4. Longitudinal velocity with EKF

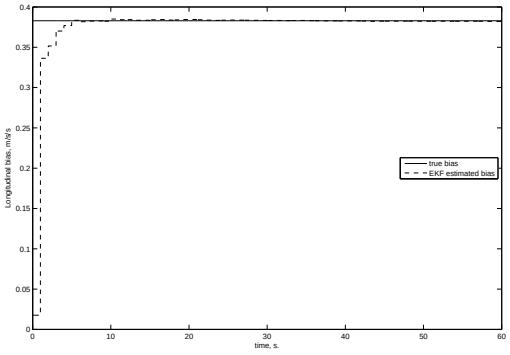

Fig. 5. Estimated bias, δ_x, in the EKF

variances of the estimated velocities over the entire time range are recorded.

Figures 6 and 7 show the error variance of longitudinal and lateral velocity, respectively, for each GPS sampling rate. The figures show clearly that the higher the sampling rate is, the less error each estimated state has. This is expected, because a higher sampling rate provides a more frequent update of GPS data every second for bias correction. As the sampling rate decreases, bias is corrected more slowly. This can be observed from the right hand linear region (1-100 Hz) in the figures. As the sampling rate decreases below 1 Hz, the absolute error starts to increase rapidly.

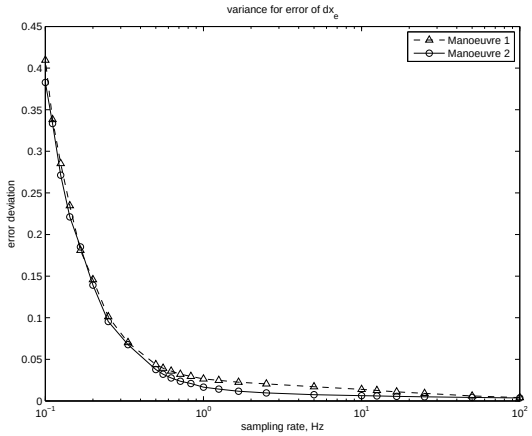

Fig. 6. Error deviation of longitudinal velocity over a range of GPS sampling rate (0.1 Hz to 100 Hz)

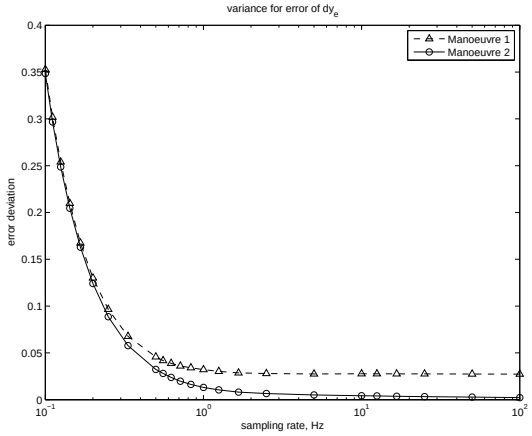

Fig. 7. Error deviation of lateral velocity over a range of GPS sampling rate (0.1 Hz to 100 Hz)

The results also show that a GPS receiver with a rate higher than 1 Hz has similar estimation error. The benefit of having a 100 Hz GPS over a 1 Hz GPS is as little as 0.01 m/s improvement in estimation. Depending on the application of the GPS and the estimation error allowed, this chart serves as a guideline to what update frequency the GPS receiver should operate at.

In addition, as shown in Figure 7, the quality of the estimations can also be affected by the type of manoeuvre. With a simple straight line manoeuvre (i.e. manoeuvre 2), the estimation error clearly has less deviation at high sampling rate. However, as the rate decreases, the effect of the manoeuvre on the estimation accuracy become less significant.

4.3 Effect of GPS variance

This section looks at the effect of the variance of the GPS signal. The simulation is carried out with different variances, described and bounded by the 3 different types of GPS as in Table 3.

As the GPS variance increases, its measurements become less accurate and the Kalman gain, K, decreases. The EKF, therefore, tends to put less weight on the innovation and begins to trust the model estimations more. This effect

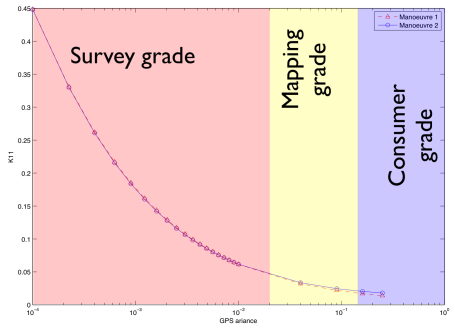

Fig. 8. Kalman gain, K_{11}, for longitudinal velocity estimation. = 1 s.

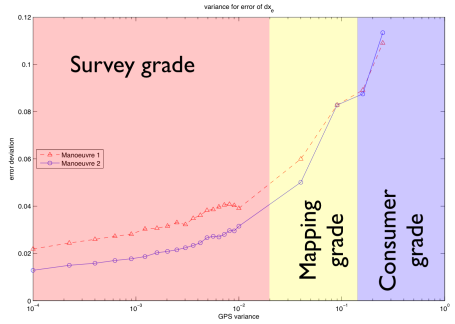

Fig. 9. Error deviation of longitudinal velocity over GPS variance (0.01 m/s to 0.5 m/s). = 1 s.

is reflected in Figure 8 where the steady state value for the longitudinal velocity decreases with the increase of GPS error. Due to the lack of confidence in the GPS, EKF has lost its primary source for correction. Bias will become harder and less accurate to predict. As a result, the error on the estimations increases.

As shown in Figures 9 and 10, the minimum estimation error deviation is achieved with the most precise GPS as would be expected. This level of error maintains before it deviates at a variance of 0.01 (SD = 0.1m/s). The two figures also indicate that the EKF in manoeuvre 2 predicts more accurately. This is because it is a simple straight line manoeuvre. As the speed of the vehicle is roughly constant (i.e. 5 m/s) throughout the simulation, the accuracy of the longitudinal velocity prediction for the two manoeuvres is similar. However, due to heavy cornering in manoeuvre 1, the lateral velocity is no longer the same for the two cases. As clearly shown in Figure 10, the error deviates more as the vehicle is cornering. When the GPS variance increases, the error deviates less for the manoeuvre where the vehicle travels on a straightroad.

Figures 9 and 10 are also subdivided into 3 regions correspond to the 3 GPS grades. It shows that low error deviations are constituted mostly by the survey grade GPS. Consumer grades have the largest deviations of all, especially when the vehicle iscornering.

The results show that estimation accuracy is more sensitive to the precision of GPS than the sampling time. As precision is directly related to the price of the receiver, this provides an extra challenge for thedesigner.

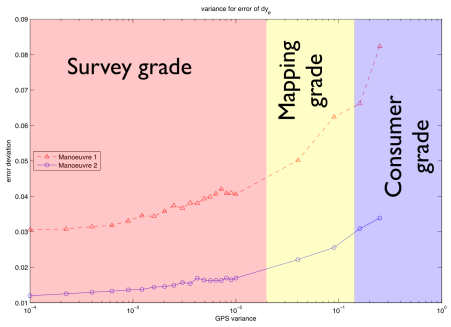

Fig. 10. Error deviation of lateral velocity over GPS variance (0.01 m/s to 0.5 m/s) . = 1 s.

5. CONCLUSIONS

Assuming perfect information from the gyro, an EKF is used to fuse the INS with the GPS. This paper has provided some quantitative data for the effect of GPS quality on EKF estimation accuracy. In order to have an effective estimation on the EKF, this paper concludes that the sampling rate of the GPS has to be greater than or equal to 1 Hz and/or the GPS variance has to be smaller than 0.01. Any sampling rate that is higher than 1 Hz only improves the error marginally. Results have also suggested that EKF estimation is sensitive to GPS variance, as well as vehicle manoeuvres. Without any cornering, state estimations are more accurately predicted.

Furthermore, this paper has given designer an idea on how to choose the type of GPS (i.e. precision and sampling rate) to suit the estimation error criterion. With suitable GPS quality, states can be predicted effectively and efficiently while INS errors are being corrected. These estimated states can be used for determining tyre slippages and validating vehicle models, thus, enhancing control and safety in different driving condition.

For future study, this paper can be be extended to real life testing with vehicle performing on different driving scenarios and maneuvers.

6. ACKNOWLEDGEMENT

The authors would like to express their thanks to Jaguar Land Rover and EPSRC for their support on this ongoing project.

REFERENCES

Anderson, R. and D.M. Bevly (2004), Estimation of slip angles using a model based estimator and GPS, *in* 'Proceedings of American Control Conference', Boston, Massachusetts.

Bevly, D.M., J. Ryu and J.C. Gredes (2006), 'Integrating INS sensors with GPS measurements for continuous estimation of vehicle sideslip, roll, and tire cornering stiffness', *IEEE Transaction on Intelligent Transportation Systems* **Vol.7**, pp.483–493.

Bevly, D.M., J.C. Gredes and C. Wilson (2002), 'The use of GPS based velocity measurements for measurement of sideslip and wheel slip', *Journal of Vehicle System Dynamics* **Vol.38**, pp.127–147.

Bhatti, U.I., W.Y. Ochieng and S. Feng (2007), 'Integrity of an integrated GPS/INS system in the presence of slowly growing errors. part ii: analysis', *GPS Solution* **Vol.11**, pp.183–192.

Cho, S.Y., B.D. Kim, Y.S. Cho and W.S. Choi (2007), 'Multi-model switching for car navigation containing low-grade imu and GPS receiver', *ETRI Journal* **Vol.29**, pp.688–690.

Gao, J., M.G. Petovello and M.E. Cannon (2007), 'Gps/low-cost imu/onboard vehicle sensors integrated land vehicle positioning system', *Journal of Embedded Systems* **Vol.2007**, ID 62616.

Grewal, M.S., L.R. Weill and A.P. Andrews (2007), *Global Positioning Systems, Inerial Navigation, and Integration*, Wiley-Interscience, Hoboken, New Jersey.

Nassar, S. and N. El-Sheimy (2006), 'A combined algorithm of improving ins error modeling and sensor measurements for accurate ins/gps navigation', *GPS Solution* **Vol.10**, pp.29–39.

Nassar, S., X. Niu and N. El-Sheimy (2007), 'Land-vehicle ins/gps accurate positioning during gps signal blockage periods', *Journal of Surveying Engineering* **Vol.133**, pp.134–143.

Wing, M.G., A. Eklund and L.D. Kellogg (2005), 'Consumer-grade global positioning system (gps) accuracy and reliability', *Journal of Forestry* **Vol.103**, pp.169–173.